



ARTICLE

Productivity Prediction Model of Perforated Horizontal Well Based on Permeability Calculation in Near-Well High Permeability Reservoir Area

Shuangshuang Zhang^{1,*}, Kangliang Guo¹, Xinchun Gao¹, Haoran Yang¹, Jinfeng Zhang² and Xing Han³

¹College of the Earth Science, Yangtze University, Wuhan, 430100, China

²PetroChina Changqing Oilfield Fifth Oil Production Plant, Xi'an, 710201, China

³Sinopec Jiangnan Oilfield Information Center, Wuhan, 430100, China

*Corresponding Author: Shuangshuang Zhang. Email: waiwai1515@163.com

Received: 03 May 2023 Accepted: 02 August 2023 Published: 27 December 2023

ABSTRACT

To improve the productivity of oil wells, perforation technology is usually used to improve the productivity of horizontal wells in oilfield exploitation. After the perforation operation, the perforation channel around the wellbore will form a near-well high-permeability reservoir area with the penetration depth as the radius, that is, the formation has different permeability characteristics with the perforation depth as the dividing line. Generally, the permeability is measured by the permeability tester, but this approach has a high workload and limited application. In this paper, according to the reservoir characteristics of perforated horizontal wells, the reservoir is divided into two areas: the original reservoir area and the near-well high permeability reservoir area. Based on the theory of seepage mechanics and the formula of open hole productivity, the permeability calculation formula of near-well high permeability reservoir area with perforation parameters is deduced. According to the principle of seepage continuity, the seepage is regarded as the synthesis of two directions: the horizontal plane elliptic seepage field and the vertical plane radial seepage field, and the oil well productivity prediction model of the perforated horizontal well is established by partition. The model comparison demonstrates that the model is reasonable and feasible. To calculate and analyze the effect of oil well production and the law of influencing factors, actual production data of the oilfield are substituted into the oil well productivity formula. It can effectively guide the technical process design and effect prediction of perforated horizontal wells.

KEYWORDS

Perforated horizontal well; permeability; productivity model; sensitivity analysis

Designation

K_1	Original formation permeability, μm^2
K_2	Permeability of perforation zone, μm^2
r_e	Supply boundary radius, m
r_w	Wellbore radius, m
r_p	Perforation radius, m
r_1	Wellbore radius converted by perforation completion, m
r_2	Wellbore radius converted by perforation completion, m
r_0	Circular isobaric radius, m



This work is licensed under a Creative Commons Attribution 4.0 International License, which permits unrestricted use, distribution, and reproduction in any medium, provided the original work is properly cited.

L_p	Perforation length (perforation depth), m
n	Perforation density, hole/m
q	Borehole well production, m ³ /d
p_{wf}	Bottom hole flowing pressure, MPa
p_e	Boundary pressure, MPa
h	Formation thickness, m
μ	Formation crude oil viscosity, mPa•s
B	Crude oil conversion coefficient, underground/ground tons
θ	Perforation phase angle
a	Horizontal elliptical seepage field long semi-axis of horizontal well, m
b	Horizontal elliptical seepage field short half axis of horizontal well, m
L	Horizontal section length of perforated horizontal well, m
Q	Perforated horizontal well productivity, m ³ /d
p_1	Boundary pressure of horizontal well near wellbore area, MPa
p_2	Circular isobaric boundary pressure, MPa
p_3	Boundary pressure of outer edge of near-well high permeability reservoir area, MPa

1 Introduction

During the advancement of oil and gas fields, perforation completion frequently serves to boost output in horizontal wells. Numerous refinements in the perforation process have been accomplished over time, enhancing the fluid passage's efficiency between the production stratum and wellbore while reducing harm to the production layer. Researchers employed a preliminary electrolytic simulation model to examine the influence of factors such as perforation length, radius, and phase angle on the productivity of wells [1,2]. The perforation may be long enough for the productivity of the perforated well to surpass that of the open hole well, according to the findings. An experiment using electrolysis equipment led to the development of the empirical equation for perforation flow efficiency.

Researchers have suggested finite difference and finite element numerical methods to get the analytical expression of perforation productivity. Hong employed the finite difference approach to acquire productivity data, concluding that the effect of perforation shape, length, and orientation on formation varies [3]. Bell et al. discovered using the finite difference method that the permeability of the compacted region surrounding the perforated hole is between 10% and -20% of the original formation [4]. McLeod et al. presented the skin of the fracture area and damage area based on simplifying the geometric perforation model and determined the productivity formula of perforated wells [5,6]. With the enhancement of computing facilities function, to assess the productivity of perforated wellbore, Roostaei et al. employed the particular finite difference algorithm for a near wellbore grid, which can readily represent various perforation configurations [7,8]. Based on a finite difference model, Zhang et al. investigated the variables affecting the permeability distribution surrounding perforated tunnels [9]. Koltz et al. were the first to assess perforation productivity with compacted zones using the finite element approach [10]. To analyze the perforation capacity with compaction zones, damaged zones surrounding wellbores, and varied phase angles between neighboring perforations, Locke et al. initially utilized a three-dimensional (3-D) model [11,12], this approach can imitate the perforation geometry more precisely. In the compacted zone surrounding the hole, McLeod et al. utilized the idea of radial turbulence and developed a straightforward model for gauging productivity [5]. Elsanoose et al. overcame the finite difference model's drawbacks by using hybrid and local mesh refining [13].

A semi-analytical model was built by Karakas et al. [14], who also proposed an empirical equation for calculating the perforation skin. He also analyzed the all-encompassing effect of formation contamination and perforation processes on the overall productivity of a well. The productivity of perforated wells under Darcy flow may be predicted using the semi-analytical model put forward by Hagoort [15]. Researchers analyzed the influence of perforation parameters based on semi-analytical models, including contaminated areas and crushed areas [16–21].

Scholars have put a lot of effort into developing a productivity prediction model for perforated horizontal wells. The seepage field and pressure drop distribution of horizontal wells were established by Borisov et al., along with several productivity forecast methods for horizontal wells [22,23]. The Joshi model is the most widely utilized among them. It primarily uses current field theory to simplify a three-dimensional seepage problem in horizontal wells to two interconnected two-dimensional seepage problems. The horizontal well productivity calculation model is generated by assuming that the oil discharge body of the horizontal well is an ellipsoid with the two ends of the horizontal section as the focus. Sognesand et al. developed a model for single-phase flow to address the issue of unequal inflow profiles in perforated horizontal wellbores [24]. A selected perforation method was chosen based on the impact of perforation compaction and others, however, the end model output was decreased. Su et al., through their experimental findings, have classified the pressure drop phenomena in horizontal wellbores into four distinct categories: pressure drop caused by friction against the tube wall, acceleration-induced pressure drop, pressure drop due to hole roughness, and pressure drop resulting from fluid mixing [25].

A coupling model of reservoir seepage and pipe flow in a wellbore was developed by Ouyang et al. [26]. The models of radial flow, axial flow, and semi-circular radiation flow were created by Li et al. using the finite element method after studying the two-dimensional analytical solution model of ideal flow [27]. Wu et al. suggested a productivity calculation method for horizontal perforated wells in low permeability reservoirs based on the three-radial flow model [16]. Liu et al. described how to create a transient calculation model for single-phase flow in horizontal wells from the perspectives of reservoir seepage, horizontal wellbore flow (using one flow as an example), and coupling model of two flows [28]. Bi et al. developed a three-dimensional unsteady productivity prediction model for horizontal wells using the finite volume approach [29]. This model may be utilized to forecast horizontal well pressure and production distribution in anisotropic reservoirs. The release impact of productivity has significant requirements on perforation parameters and reservoir parameters data during the perforated horizontal well completion process. Through a wide range of tests and techniques, researchers have explored productivity, skin factor, and seepage law. The choice of perforation technique and the productivity release are both influenced by various perforation parameters in distinct ways.

The model described in this paper is an oil well productivity prediction model based on the permeability calculation of near-well high permeability reservoir area. This refers to a method not incorporated in any of the existing models. The permeability in the model calculation was previously assessed by the permeability tester, however, this approach has a high workload and limited application.

During the perforation process, the perforating bullet will leave a perforation channel in the near-well reservoir area. The perforation channel will generate a near-well high-permeability reservoir area with the penetration depth as the radius around the wellbore, forming different permeability reservoir characteristics with the perforation depth as the dividing line. This paper constructs the permeability calculation formula of a perforated horizontal well near a well high permeability reservoir area

using fluid mechanics theory and open hole productivity formula. The capacity prediction model is constructed in partition using the theories of disturbed elliptical flow and radial flow. The comparison of models validates the research's methodology, proving it to be both rational and applicable. It is concluded that the oil well productivity formula can not only significantly reduce working time and calculation error, but also adeptly steers the technical process design and outcome forecasting for perforated horizontal wells. Moreover, it bolsters economic advantages for oilfield development.

2 Methodology

Near-well stimulation measures are commonly applied to enhance oil well productivity when oilfields are exploited. Typically, the perforation stimulation technique is utilized to improve horizontal well production. The perforating bullet will create a perforation channel in the near-well reservoir region during the perforation process, and the channel will surround the wellbore in a radius of penetration depth to create a near-well high-permeability reservoir area.

The main content of this chapter is: that the reservoir is divided into two regions based on the reservoir characteristics of perforated horizontal wells: the original reservoir area and the near-well high permeability reservoir area. (1) After building a mathematical geometric model, a formula is used to determine the wellbore radius r_1 of the perforation completion. The open hole completion productivity formula is constructed in combined with the principle of fluid seepage continuity; Then the mathematical formula to convert another wellbore radius r_2 and bring it into the open hole completion productivity formula; Using the productivity formula of open hole completion as a bridge, the relationship between the ratio of perforation zone permeability to the original formation permeability and perforation parameters is deduced, and the expression K_2 of perforation zone permeability is obtained. (2) Seepage is regarded as the synthesis of flow in two directions: the horizontal elliptical seepage field and the vertical radial seepage field, and the productivity prediction model of the perforated horizontal well is established by partition. (3) The model proposed in this paper is compared with the Joshi model, Karakas model, and McLeod model. The whole process is shown in Fig. 1.

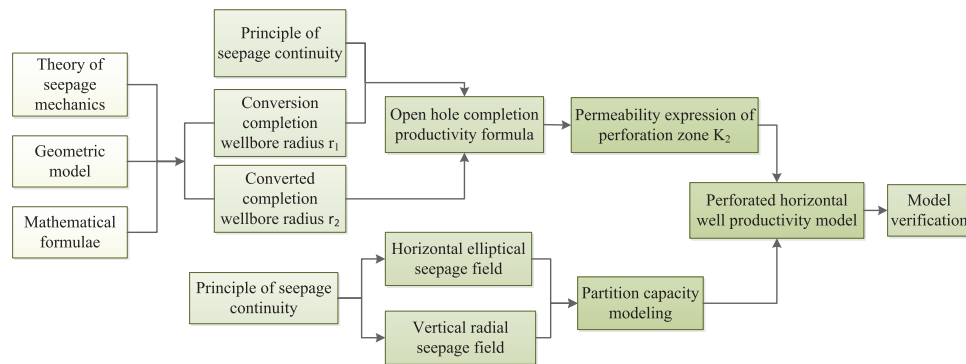
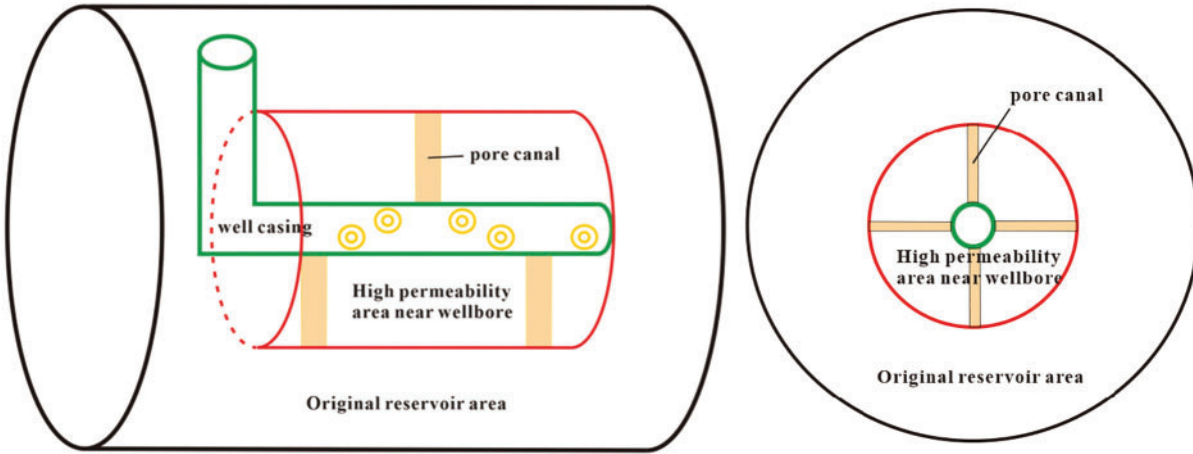


Figure 1: Research method flow diagram

To begin, some assumptions must be made when constructing the steady-state flow productivity formula: the perforated well is an ideal horizontal well, and the formation is a single-layer and constant-thickness column; the fluid within the reservoir exhibits single-phase, incompressible flow characteristics, primarily in the form of laminar flow; and the supply radius is much larger than the sum of wellbore radius and perforation depth [14,21,30].

The pore distribution map presented in Fig. 2 is constructed in three-dimensional space. Fig. 2a indicates that the improved near-well high permeability reservoir area is within the range of perforation depth, but the original reservoir area is outside the range of perforation depth. The profile of the horizontal section of the wellbore is shown in Fig. 2b, and the reservoir model with differed permeability is produced by taking the perforation depth as the dividing line. That is, the reservoir of a perforated horizontal well is divided into two regions: one is the original reservoir region, and the other is the near-well high permeability reservoir region.



(a) Perforated horizontal well pore distribution diagram (b) Wellbore horizontal section profile diagram

Figure 2: Schematic diagram of reservoir physical model

2.1 Permeability Calculation Formula of Perforation Zone

The perforation channel is considered to be a regular cylinder [14,30,31], and the wellbore is likewise assumed to be a normal cylinder, as illustrated in Fig. 3. The open area of the open-hole completion (well diameter r_1) is A_1 , and the open area of the open-hole completion (well diameter r_2) is A_2 ; the opening area of the perforation completion foundation is B_1 , the whole opening area of the perforation completion is B_2 ; the upper bottom area of the perforated hole is C_1 , and the side area of the perforated hole is C_2 . The relationship is computed according to the cylindrical geometric area formula.

1. The open area of open hole completion is regarded as the open area of the perforation completion foundation, and the upper bottom area of the perforation hole is regarded as the open area of the perforation completion foundation. The equation can be obtained:

$$\begin{cases} A_1 = 2\pi r_1 h \\ C_1 = \pi r_p^2 n h \\ A_1 = C_1 = B_1 \end{cases} \quad (1)$$

The wellbore radius r_1 converted by the perforation completion is obtained:

$$r_1 = \frac{n}{2} r_p^2 \quad (2)$$

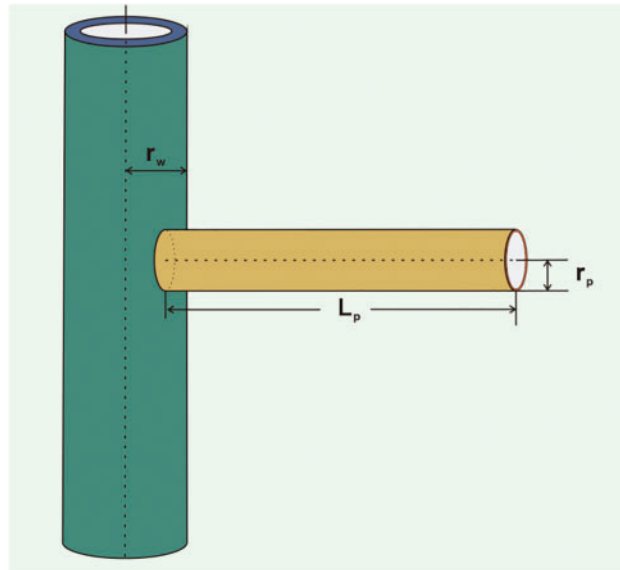


Figure 3: Wellbore-perforated hole geometric model diagram

The formation permeability in the perforation zone differs from the initial formation permeability as a result of the action of perforation. The formation may be separated into an original formation region and a high permeability area near the well perforation, with permeabilities of K_1 , K_2 . According to the continuity principle of fluid seepage in strata, the open hole well productivity formula may be produced by inserting r_1 (The productivity equations showcased in this article are all anchored on the practical units utilized in the International System (SI) of mineral production):

$$q = \frac{2\pi K_1 h (p_e - p_{wf})}{\mu B \ln \left(\frac{r_e}{r_w + L_p} \right)} + \frac{2\pi K_2 h (p_e - p_{wf})}{\mu B \ln \left(\frac{r_w + L_p}{r_1} \right)} \quad (3)$$

2. The open area of open hole completion is regarded as the whole open area of perforation completion, and the whole open area of perforation completion is regarded as the sum of the side area of the perforation hole and the bottom area of the perforation hole. The equation can be obtained:

$$\begin{cases} A_2 = B_2 \\ B_2 = C_1 + C_2 \\ A_2 = 2\pi r_2 h \\ C_1 = \pi r_p^2 n h \\ C_2 = 2\pi r_p L_p n h \end{cases} \quad (4)$$

The wellbore radius r_2 converted by the perforation completion is obtained:

$$r_2 = \frac{n}{2} r_p^2 + n r_p L_p \quad (5)$$

Substitute r_2 into the productivity formula of open-hole wells to obtain:

$$q = \frac{2\pi K_1 h (p_e - p_{wf})}{\mu B \ln\left(\frac{r_e}{r_2}\right)} \tag{6}$$

From Eqs. (2), (3), (5), and (6), we have:

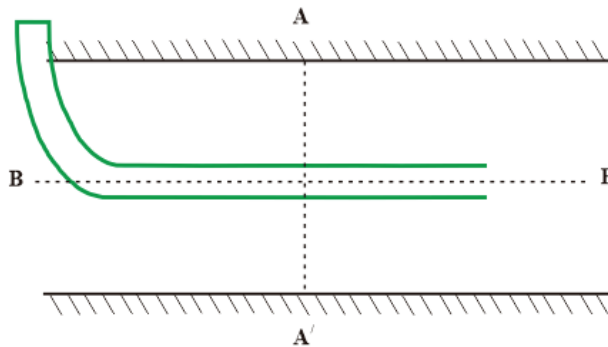
$$\frac{K_2}{K_1} = \frac{\ln\left(\frac{r_w + L_p}{\frac{n}{2}r_p^2}\right)}{\ln\left(\frac{r_w + L_p}{\frac{n}{2}r_p^2 + nr_p L_p}\right)} \tag{7}$$

$nr_p L_p \geq 0$, then $K_2/K_1 \geq 1$, demonstrating a difference in the permeability of the formation before and after perforation. The calculation formula of the perforation zone (near-well high permeability reservoir area with penetration depth as radius) permeability is:

$$K_2 = K_1 \frac{\ln\left(\frac{r_w + L_p}{\frac{n}{2}r_p^2}\right)}{\ln\left(\frac{r_w + L_p}{\frac{n}{2}r_p^2 + nr_p L_p}\right)} \tag{8}$$

2.2 Perforated Horizontal Well Productivity Model

Based on Joshi model [23], the seepage field of the fluid around the horizontal well is equivalently decomposed in the process of formulating the productivity equation for perforated horizontal wells presented in this paper, and the three-dimensional flow mode is transformed into a two-dimensional flow model, yielding two continuous seepage fields-horizontal plane elliptic seepage field and vertical plane radial seepage field, as illustrated in Fig. 4. Calculating the flow rates in two planes separately results in the productivity of perforated horizontal wells.



(a) Simplified well structure diagram

Figure 4: (Continued)

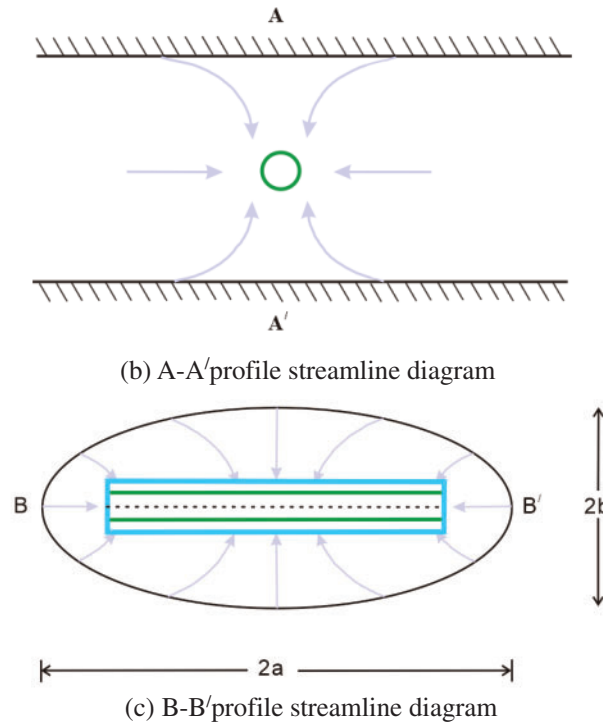


Figure 4: Horizontal well flow geometry diagram

1. Calculation of flow in horizontal elliptical seepage field

On the horizontal plane, the fluid surrounding the well flows in an elliptical flow from the reservoir supply edge to the near-wellbore area of the horizontal well, Fig. 4c. The horizontal well's near-wellbore region is depicted in Fig. 4c as a light blue rectangle. The pressure boundary is expressed as p_1 . Its breadth is equal to the thickness h of the oil layer, and its length is equal to the horizontal well's length L .

The meaning expressed in Fig. 5 is that the elliptic flow can be converted into a plane radial flow, which is convenient for the expression of the productivity formula. The elliptical area exists in the Z plane, and the midway of the horizontal well's symmetrical center, which is dispersed throughout the long axis. The long half-axis of the plane is a , and the short half-axis is b . Transforming it to the ω plane, a circular plane can be obtained, and the new plane radius is $2(a+b)/L$. In the new area, the horizontal well section $(-L/2, 0)$ $(L/2, 0)$ is mapped into the unit circle. At this time, the horizontal well with a length of L in the Z plane is converted into a vertical well with a radius of 1 in the ω plane, and the elliptical flow is converted into a planar radial flow in a finite circular reservoir with an outer boundary of $2(a+b)/L$.

According to the property of the ellipse: $b = \sqrt{a^2 - (L/2)^2}$, the inner and outer boundaries are 1, $2(a+b)/L$, respectively.

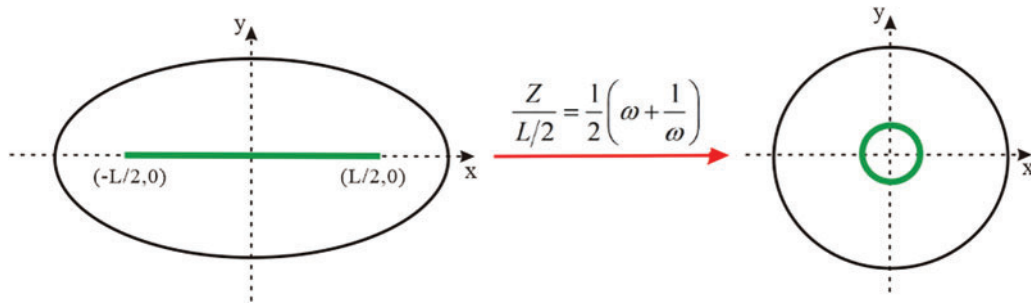


Figure 5: Horizontal elliptic seepage field transformation diagram of perforated horizontal well

The horizontal in-plane productivity formula of perforated horizontal wells can be expressed as:

$$p_e - p_1 = \frac{\mu BQ}{2\pi K_1 h} \ln \frac{2(a+b)}{L} \tag{9}$$

2. Calculation of flow in vertical radial seepage field

On the vertical section, there is a seepage field flowing from the near wellbore area to the bottom of the horizontal well, as shown in Fig. 4b. Fig. 6 also shows the seepage field of the fluid flowing to the bottom of the well on the vertical section, but the fluid flow form is subdivided into three parts, which is helpful for the expression of the productivity formula:

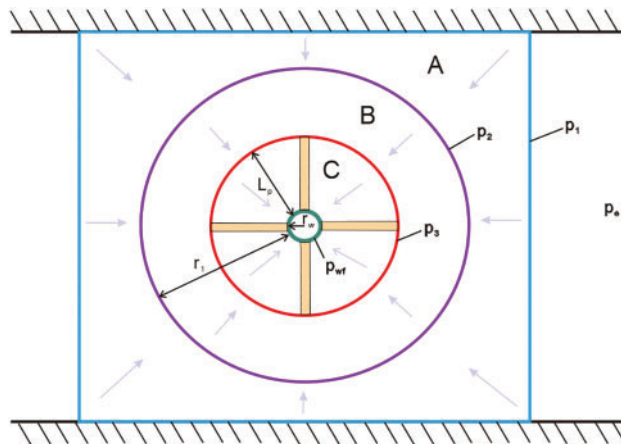


Figure 6: Perforated horizontal well vertical seepage field diagram

In Area A, which is a horizontal well near the well area, the fluid flows from the nearby well area to the circular isobaric border. The light blue rectangular line is near the well boundary, and its length and width are the oil layer thickness h . The purple circle line represents an isobaric boundary, and the pressure is expressed as p_2 . Conformal transformation is used to obtain the circular isobaric boundary. The model establishment procedure will remove the circular isobaric radius r_o .

At this time, when flowing from the near well area to the circular isobaric boundary, the productivity formula may be written as follows:

$$p_1 - p_2 = \frac{\mu BQ}{2\pi K_1 L} \ln \frac{h}{\sqrt{\pi} r_o} \tag{10}$$

Block B is the transition zone from the near well area to the perforation high permeability reservoir area. The fluid flows from the circular isobaric boundary to the outer edge of the near-well high-permeability reservoir area. The red circle line represents the outer boundary of the near-well high-permeability reservoir area. Its radius is determined by the perforation depth L_p , and the pressure is expressed as p_3 .

The productivity equation may now be written as follows when flowing from the circular isobaric boundary to the region of the near-well high-permeability reservoir:

$$p_2 - p_3 = \frac{\mu B Q}{2\pi K_1 L} \ln \frac{r_0}{L_p} \quad (11)$$

In region C, which is a high permeability reservoir area of perforated horizontal wells, the fluid travels from the outside border of the near-well high permeability reservoir region to the bottom hole. The wellbore is represented by the green circle, and the wellbore pressure is p_{wf} .

Currently, the flow from the near-well high-permeability reservoir area to the bottom hole, and the productivity formula may be represented as follows:

$$P_3 - P_{wf} = \frac{\mu B Q}{2\pi K_2 L} \ln \frac{L_p}{r_w} \quad (12)$$

The seepage equation of the perforated horizontal well may be determined by adding the flow formula of the horizontal elliptical seepage field to the flow formula of the vertical radial seepage field:

$$p_e - p_{wf} = \frac{\mu B Q}{2\pi} \left(\frac{1}{K_1 h} \ln \frac{2(a+b)}{L} + \frac{1}{K_1 L} \ln \frac{h}{\sqrt{\pi} L_p} + \frac{1}{K_2 L} \ln \frac{L_p}{r_w} \right) \quad (13)$$

The flow rates from the supply boundary to the near-wellbore area, the near-wellbore area to the circular isobaric boundary, the circular isobaric boundary to the outer edge of the near-wellbore high-permeability reservoir area, and the near-wellbore high-permeability reservoir area to the wellbore are all equal according to the principle of fluid seepage continuity. Perforated horizontal well productivity equation can be changed into:

$$Q = \frac{2\pi (p_e - p_{wf})}{\mu B \left(\frac{1}{K_1 h} \ln \frac{2(a+b)}{L} + \frac{1}{K_1 L} \ln \frac{h}{\sqrt{\pi} L_p} + \frac{1}{K_2 L} \ln \frac{L_p}{r_w} \right)} \quad (14)$$

$$\text{where: } K_2 = K_1 \frac{\ln \frac{r_w + L_p}{\frac{n}{2} r_p^2}}{\ln \frac{r_w + L_p}{\frac{n}{2} r_p^2 + n r_p L_p}}$$

2.3 Model Verification

Models developed by Karakas et al. [14] and McLeod et al. [5] show strong representativeness in perforated well productivity calculation models. These two models are reliable and accurate for calculating actual productivity. The Joshi [23] model is true and dependable for actual calculation results in the horizontal well productivity calculation model. As a result, we compare the proposed model's errors for calculating productivity to those of the Joshi, Karakas, and McLeod models. We substitute the basic parameters from Table 1 into each model.

Table 1: Basic reservoir parameters calculated based on four different models

Parameter	Numerical value
Reservoir boundary pressure p_c /MPa	30
Wellbore pressure p_{wf} /MPa	18
Formation volume coefficient	1.084
Viscosity μ /mPa•s	5
Reservoir thickness h /m	20
Wellbore radius r_w /m	0.12
Horizontal elliptical seepage field long semi-axis of horizontal well a /m	150
Horizontal section length L /m	200
Perforation radius r_p /mm	7
Perforation depth L_p /m	0.8
Perforation density n /hole•m ⁻¹	20
Perforation phase angle Θ /°	90
Crushed-zone radius r_c /mm	12
Damaged-zone radius r_d /m	0.7
Original formation permeability K_1 /mD	150
Permeability of damaged area k_d /mD	40

From the curve of pressure difference and productivity change in Fig. 7, it can be seen that the calculation results of the model in this paper are more consistent with the Karakas model and the McLeod model, and the error is very small. There is a gap in the curve distribution of the Joshi model, and the error is large. Table 2 shows the productivity and error values of the four models when the pressure difference is 6, 12, 18 MPa.

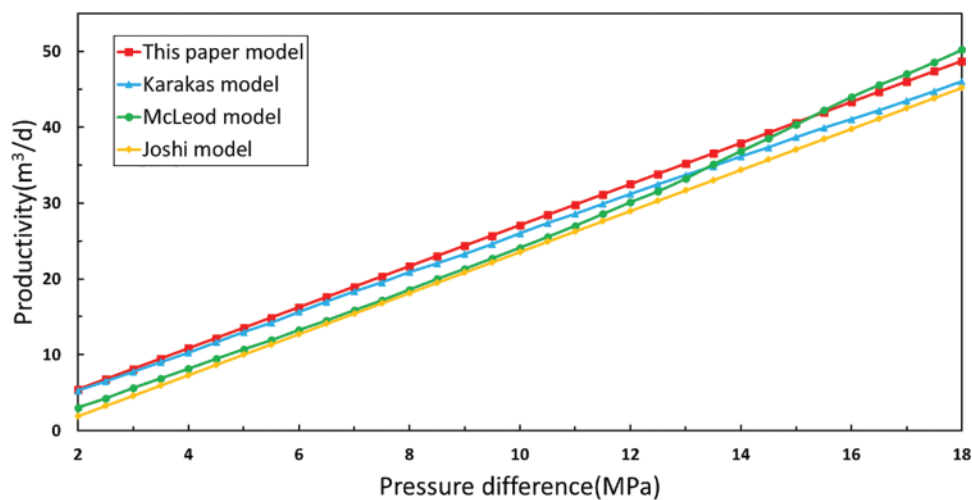


Figure 7: Pressure difference-productivity change curves calculated based on four different models

Table 2: The productivity values and error values of the four models under different pressure differences

		This paper model	Joshi model	Karakas model	McLeod model
Pressure difference (6 MPa)	Productivity (m ³ /d)	16.24	12.74	15.62	13.26
	Error magnitude (%)	–	27.47	3.97	22.47
Pressure difference (12 MPa)	Productivity (m ³ /d)	32.48	28.98	31.18	30.12
	Error magnitude (%)	–	12.08	4.17	7.84
Pressure difference (18 MPa)	Productivity (m ³ /d)	48.72	45.22	46.02	50.23
	Error magnitude (%)	–	7.74	5.89	–3.01
Average magnitude of error (%)		–	15.76	4.68	9.1

The average error between the model in this paper and the Joshi model is 15.76%, and the error value is high. This is because the Joshi model is a horizontal well production calculation formula that does not include perforation parameters. If the Joshi model is still employed after the horizontal well has been perforated, the calculation result will be lesser. However, both the Karakas and McLeod models are used to predict the productivity of perforated wells, and the average error of productivity calculation between this model and the Karakas and McLeod models is 4.68% and 9.1%, respectively. This indirectly demonstrates the reasonableness and feasibility of the presented model. Therefore, the model can be used to calculate the productivity of perforated horizontal wells.

3 Discussion and Analysis

The field data of an oil well are substituted into the model for calculation to verify its reliability and practicability. The detailed well parameters are shown in Table 3. Table 4 displays the well's calculated and actual production for the test segment. The difference between the production capacity calculated by the model and the actual test capacity is 3.26%, and the error is very small. This suggests that the model may be used for the investigation of injection hole parameters and reservoir capacity calculations for well completion.

Table 3: Basic parameters of a measured well

Parameter	Numerical value
Reservoir boundary pressure p_e /MPa	32.376
Wellbore pressure p_{wf} /MPa	20.201
Formation volume coefficient	1.056
Viscosity μ /mPa•s	5
Reservoir thickness h /m	20
Wellbore radius r_w /m	0.11025
Horizontal elliptical seepage field long semi-axis of horizontal well a /m	400
Horizontal section length L /m	500

(Continued)

Table 3 (continued)

Parameter	Numerical value
Perforation radius r_p /mm	0.0109
Perforation depth L_p /m	0.913
Perforation density n /hole•m ⁻¹	40
Original formation permeability K_1 /mD	0.15

Table 4: Comparison table of measured results and model results

	Productivity (m ³ /d)	Error magnitude (%)
Practical testing	36.268	–
Model calculation in this paper	37.449	3.26

The curve of the productivity and perforation parameters of the perforated well is produced by providing the perforation parameters, using the model calculation Eq. (14), and the sensitivity analysis is completed. It is assumed that the perforation density is 8–40 holes/m, the perforation depth is 0.15–1.05 m, the perforation radius is 3–21 mm, and the perforation wellbore radius is 0.108 m.

When the perforation density is 16 holes/m under the condition of other formation parameters, Fig. 8 displays the change curve of the influence of hole depth-radius on the productivity of perforated wells. The two maps may be compared to show that the hole depth is more sensitive to productivity than the perforation radius. The perforation depth is a significant factor impacting production, as is seen in Fig. 8a. With deeper perforations, perforated wells become more productive. However, when the hole depth increases to a certain value, the production capacity will not increase too much by increasing the hole depth. As illustrated in Fig. 8b, the releasing impact of various pore size values on perforation productivity is not immediately apparent when the hole depth is less than 45 cm. When the hole depth exceeds 45 cm, productivity steadily rises with increasing perforation radius once the hole depth takes a certain value. However, the distribution of the curve shows that as the hole radius increases, the rate of productivity growth eventually decreases. The rationale for this is that, based on field construction experience, a big aperture will reduce casing strength and shorten casing service life. Therefore, an appropriate radius may be chosen throughout the building process. The hole radius of the projectile used in field construction has a small range of variation at the moment. Because the explosive quantity and energy of the perforating projectile are constant, there is a tendency for it to trade a smaller hole radius (around 10 mm) in favor of a deeper hole.

When the perforation radius is 9 mm under the condition of other formation parameters, Fig. 9 displays the change curve of the influence of hole depth density on the productivity of perforated wells. The capacity of perforated wells is enhanced as the depth and density of the holes expand, however, it is clear from a comparison of the two maps that hole depth is more sensitive to productivity than hole density. When the perforation depth is limited, increasing the hole density can enhance the productivity release effect. As can be observed, a significant parameter affecting the production ratio is the hole density. Yet, the hole density cannot be raised indefinitely. Several factors must be taken into account: hole density is too large to cause casing damage; the hole density is too large and the perforation cost is high; too large hole density will complicate the construction work. A means to choose an optimal hole density should be based on the conditions of oil and gas wells and other perforation factors during

perforation construction. Combined with the choice of hole depth, the perforation technique with a large penetration depth performs better than the method with a large hole density, in oil and gas wells with drilling or workover and perforation damage.

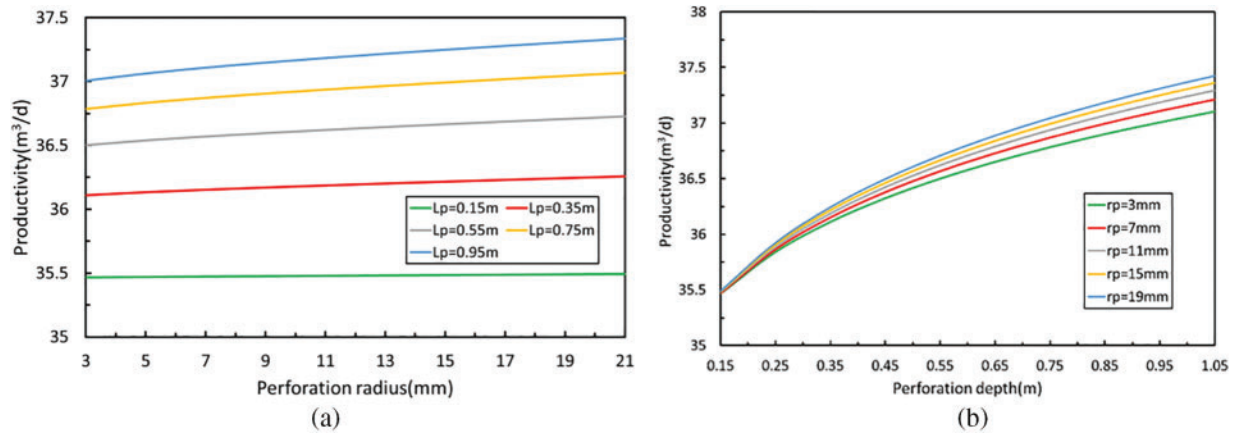


Figure 8: The change diagram of the influence of perforation depth-radius on productivity

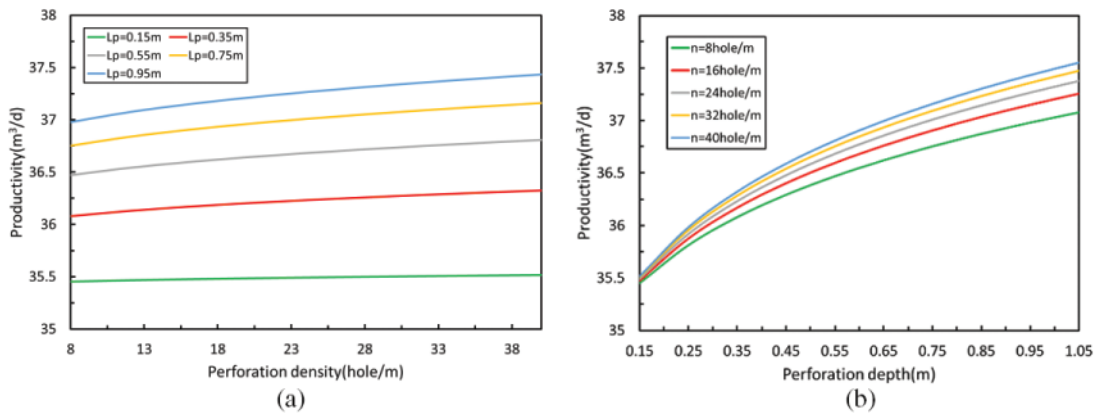


Figure 9: The change diagram of the influence of perforation depth-density on productivity

Whenever the perforation depth is 0.75 m under the condition of other formation parameters, Fig. 10 displays the graph of the fluctuation of the influence of pore radius density on the productivity of perforated wells. As pore radius and density grow, perforated well productivity also rises, although as can be seen from a comparison of the curve inclination angles in the two maps, pore density is more sensitive to productivity than pore radius. Fig. 10a demonstrates that the productivity growth when the hole density is less than 24 holes/m is much slower than when the hole density is larger than 24 holes/m. Fig. 10b shows that when the aperture is less than 20 mm, the capacity growth is much smaller than when the aperture is higher than 20 mm. In contrast to field construction, a big perforation radius will reduce the casing strength and shorten its service life. The hole radius is frequently constrained when the process is selected. At this point, increasing the hole density will improve the perforation effect.

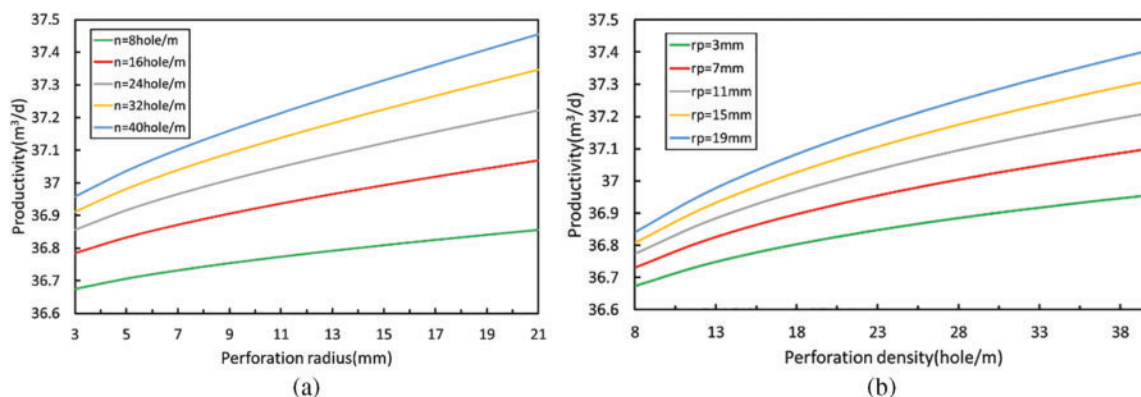


Figure 10: The change diagram of the influence of perforation radius-density on productivity

In summary, the whole depth of penetration is a crucial element impacting productivity, and the relationship with productivity varies depending on the circumstances. The productivity of perforated oil wells is somewhat influenced by the depth, density, and radius of the holes. Hole depth has the greatest impact, followed by hole density and pore size. The sensitivity analysis of perforation parameters on productivity has led to the conclusion that, when selecting a perforation technique, greater perforation parameters have a higher productivity release impact. Nevertheless, considering that the excessive perforation parameters will lead to the damage of casing strength and shorten the service life, a perforation method with a pore radius of around 10 mm and a pore density of 24–40 holes/m.

4 Summary and Conclusion

The reservoir is separated into two parts in this research based on the reservoir characteristics of perforated wells: the original reservoir area and the near-well high permeability reservoir area. The following findings have been reached:

1. Based on the principle of seepage mechanics, the calculation formula of the permeability of the perforated near-well high permeability reservoir area with parameters such as hole depth, hole density, and pore radius, is derived in this paper by constructing the mathematical geometric model and using the open hole completion productivity formula.
2. In this paper, according to the principle of seepage continuity, the seepage of a perforated horizontal well is regarded as the synthesis of two directions: the elliptic seepage field in the horizontal plane and the radial seepage field in the vertical plane, and the productivity formula of the perforated horizontal well is established by partition. According to the model calculation and comparison, the average error between this model and the Karakas model is 4.68%, and the average error between this model and the McLeod model is 9.1%, which indirectly shows the model's rationality and applicability.
3. According to the findings of a productivity sensitivity analysis of perforated horizontal wells, the hole depth, hole density, and hole radius, all contribute to influencing the productivity of perforated oil wells. The biggest effect is exerted by hole depth, followed by hole density and hole radius. To minimize casing strength loss due to too big an aperture, perforation depth and density should be prioritized in process technology selection.
4. Based on the oil well productivity formula derived in this paper, a systematic perforation parameter optimization method is formed by studying the constraint relationship between

perforation parameters, which can efficiently steer the technical design and predict the outcome of perforated horizontal wells.

Acknowledgement: The authors deeply appreciate the backing provided by Yangtze University for this research. They also wish to extend their gratitude to Professor Guo Kangliang for his insightful interpretation of the study's findings.

Funding Statement: The authors received no specific funding for this study.

Author Contributions: The authors confirm their contribution to the paper as follows: study conception and design: Shuangshuang Zhang, Kangliang Guo, data collection: Xincheng Gao, Jinfeng Zhang; analysis and interpretation of results: Shuangshuang Zhang, Kangliang Guo, Haoran Yang; draft manuscript preparation: Shuangshuang Zhang, Xing Han. All authors reviewed the results and approved the final version of the manuscript.

Availability of Data and Materials: The raw data supporting the conclusions of this article will be made available by the authors, without undue reservation.

Conflicts of Interest: The authors declare that they have no conflicts of interest to report regarding the present study.

References

1. Muskat, M. (1943). The effect of casing perforations on well productivity. *Transactions of the AIME*, 151(1), 175–187.
2. McDowell, J. M., Muskat, M. (1950). The effect on well productivity of formation penetration beyond perforated casing. *Journal of Petroleum Technology*, 2(11), 309–312.
3. Hong, K. C. (1975). Productivity of perforated completions in formations with or without damage. *Journal of Petroleum Technology*, 27(8), 1027–1038.
4. Bell, W. T., Brieger, E. F., Harrigan Jr, J. W. (1972). Laboratory flow characteristics of gun perforations. *Journal of Petroleum Technology*, 24(9), 1095–1103.
5. McLeod Jr, Harry, O. (1983). The effect of perforating conditions on well performance. *Journal of Petroleum Technology*, 35(1), 31–39.
6. Abobaker, E. E., Elsanouse, A., Khan, F., Rahman, M. A., Aborig, A. (2022). A new assessment of perforation skin factor for vertical perforated wells in near-wellbore region. *Journal of Petroleum Exploration and Production Technology*, 12, 117–133.
7. Roostaie, M., Soroush, M., Mohammadtabar, F., Mohammadtabar, M. (2021). Design for reliability: Experimental and numerical simulation of cased and perforated completions with standalone screen. *SPE Drilling & Completion*, 36(3), 680–706.
8. Dogulu, Y. S. (1998). Modeling of well productivity in perforated completions. *SPE Eastern Regional Meeting*, SPE-51048-MS. Pennsylvania, USA.
9. Zhang, Z., Guo, J., Liang, H., Liu, Y. (2021). Numerical simulation of skin factors for perforated wells with crushed zone and drilling-fluid damage in tight gas reservoirs. *Journal of Natural Gas Science and Engineering*, 90, 103907.
10. Klotz, J. A., Krueger, R. F., Pye, D. S. (1974). Effect of perforation damage on well productivity. *Journal of Petroleum Technology*, 26(11), 1303–1314.
11. Locke, S. (1981). An advanced method for predicting the productivity ratio of a perforated well. *Journal of Petroleum Technology*, 33(12), 2481–2488.

12. Sadrnejad, S. A., Ghasemzadeh, H., Khodaei Ardabili, A. (2018). A finite element model for simulating flow around a well with helically symmetric perforations. *Journal of Engineering Geology*, 12, 159.
13. Elsanoose, A., Abobaker, E., Khan, F., Rahman, A., Aborig, A. (2021). Investigation of multiphase flow in porous media around perforation tunnel near wellbore region, experimental and numerical study. *ASME 2021 40th International Conference on Ocean, Offshore and Arctic Engineering*, vol. 10, V010T11A040.
14. Karakas, M., Tarlq, S. M. (1991). Semianalytical productivity models for perforated completions. *SPE Production Engineering*, 6(1), 73–82.
15. Hagoort, J. (2007). An analytical model for predicting the productivity of perforated wells. *Journal of Petroleum Science and Engineering*, 56(4), 199–218.
16. Wu, M., Zhu, J., Li, L., Li, P. (2020). Calculation of perforated vertical and horizontal well productivity in low-permeability reservoirs. *SPE Drilling & Completion*, 35(2), 218–236.
17. Zhao, J., Chen, X., Li, Y., Fu, B., Xu, W. (2017). Numerical simulation of multi-stage fracturing and optimization of perforation in a horizontal well. *Petroleum Exploration and Development*, 44(1), 119–126.
18. Mohammed, H. S., Khazal, E. A., Sultan, H. S. (2020). Studying the effect of perforation parameters on vertical well performance. *Basrah Journal for Engineering Sciences*, 20(2), 84–59.
19. Mohammed, H. S., Sultan, H. S., Khazal, E. A. (2022). Simulation of a perforated vertical wellbore with near wall porous media effect. *Journal of Petroleum Research and Studies*, 12(1), 85–104.
20. Grove, B., Grader, A., Derzhi, N. (2019). Perforation damage, cleanup, and inflow performance: Advances in diagnostics and characterization. *SPE Middle East Oil and Gas Show and Conference*, D041S039R002. Pennsylvania, USA.
21. Abobaker, E., Elsanoose, A., Khan, F. (2021). Comparison of crushed-zone skin factor for cased and perforated wells calculated with and without including a tip-crushed zone effect. *Geofluids*, 2021(2), 1–13.
22. Borisov, J. P. (1984). *Oil production using horizontal and multiple deviation wells*. Bartlesville: The R&D Translation Company.
23. Joshi, S. D. (1988). Augmentation of well productivity with slant and horizontal wells. *Journal of Petroleum Technology*, 40(6), 729–739.
24. Sognesand, S., Skotner, P., Hauge, J. (1994). Use of partial perforations in Oseberg horizontal wells. *SPE Annual Technical Conference and Exhibition*, SPE-28569-MS. Anaheim, CA, USA.
25. Su, Z., Gudmundsson, J. S. (1994). Pressure drop in perforated pipes: Experiments and analysis. *SPE Asia Pacific Oil and Gas Conference*, SPE-28800. Adelaide, Australia.
26. Ouyang, W., Yang, D., Sun, H. (2020). Transient pressure analysis in partially perforated vertical wells. *Proceedings of the International Field Exploration and Development Conference*, pp. 873–891. Chengdu, China.
27. Li, H., Tan, Y., Jiang, B. (2018). A semi-analytical model for predicting inflow profile of horizontal wells in bottom-water gas reservoir. *Journal of Petroleum Science and Engineering*, 160, 351–362.
28. Liu, P., Wang, Q., Luo, Y. (2022). Study on a new transient productivity model of horizontal well coupled with seepage and wellbore flow. *Processes*, 9(12), 2257.
29. Bi, G., Cui, Y., Wu, J. (2022). Unsteady Productivity prediction for three-dimensional horizontal well in anisotropic reservoir. *Geofluid*, 2022, 2697311.
30. Abobaker, E., Elsanoose, A., Khan, F., Rahman, M. A., Aborig, A. (2021). A new evaluation of skin factor in inclined wells with anisotropic permeability. *Energies*, 14(17), 5585.
31. Satti, R. P., Bale, D. S., Zuklic, S. N., Koliha, N., Crouse, B. (2017). Digital rock simulation: A novel approach for accurate characterization of perforation tunnel damage. *SPE Western Regional Meeting*, D041S015R003. Pennsylvania, USA.